TRANSMUTATION CAPABILITY OF ONCE-THROUGH CRITICAL OR SUB-CRITICAL MOLTEN-SALT REACTORS

Elena Rodriguez-Vieitez, Micah D. Lowenthal,[1] **Ehud Greenspan** and **Joonhong Ahn**
Department of Nuclear Engineering,
University of California,
Berkeley, CA 94720-1730, USA
ervieitez@nuc.berkeley.edu, gehud@nuc.berkeley.edu

Abstract

A neutronic parametric study is performed for graphite-moderated molten-salt (MS) critical or source-driven sub-critical transmuting reactors. The NaF-ZrF_4 MS reactor is fuelled with transuranium isotopes from LWR spent fuel and operates in a once-through mode. The MS with actinides is continuously fed and continuously extracted at a very slow rate. All the fission products are removed from the core as soon as formed. The primary question addressed is whether or not it is possible to design such a reactor to have an acceptable k_{eff} when at equilibrium composition, while the Ac concentration is below their solubility limit, and what is the corresponding transmutation fraction. The primary design variables are the MS channel diameter and the graphite-to-MS volume ratio (C/MS). For an average power density of 390 W/cm^3 of MS, MS feed rate of 1 millilitre/day/MW_{th} and actinide concentration of 12.87 mol% it was found that both k_{eff} and the fractional transmutation peak while the equilibrium concentration is at a minimum when C/MS is close to 1.0. The equilibrium actinide concentration is below the solubility limit for C/MS between 1 and 7 for 7cm and 3.5 cm channel diameter and between 1 and 15 for a 1 cm channel diameter. The peak k_{eff} is close to 1.0 and the fractional transmutation exceeds 90% in one pass through the core. The Pu coming out from the C/MS=12 core has a very low fissile content of only 17%. The optimal core has an epithermal spectrum and small channel diameter. The graphite lifetime in the core is 0.6 or 1.3 years for C/MS of 1 or 3, respectively. Reduction of the power density to 39 W/cm^3 can increase the graphite lifetime by an order of magnitude. This reduction of the power density reduces the attainable k_{eff} by ~5% and increases the equilibrium actinide concentration by ~0.4 mol%. An illustrative core design for a 10 GW_{th} MS transmuter is given.

1. Present address: National Research Council, Washington DC.

1. Introduction

The transmutation capability of graphite-moderated molten-salt (MS) reactors is being studied at the University of California, Berkeley in the framework of the University Programme of the US DOE ATW project. [1] A previous parametric study of MS reactors [2,3] did not account for the solubility limits of actinides (Ac) and fission products (FP) in the $NaF:ZrF_4$ molten-salt. One objective of the present research is to extend this analysis to take into account the solubility limits of actinides (Ac). Another objective is to find the optimal neutron spectrum for a MS transmuting reactor.[2] An additional objective is to work out an illustration of a core design for a high-performance MS reactor.

The MS transmuter concept being considered is described in Section 2. The study variables and constraints are discussed in Section 3. The model used for calculating the MS reactor neutronics is described in Section 4 followed by a summary of the obtained results (Section 5) and a discussion (Section 6).

2. Reference molten-salt reactor

The reference design for the MS reactor concept considered in this work is the ADNA Tier-I reactor concept proposed by Bowman. [4] The reactor is an accelerator-driven assembly made up of a 400 cm tall block of graphite, roughly 400 cm across, penetrated by 7 cm diameter channels at a hexagonal pitch of approximately 30 cm, through which the molten-salt fuel flows. The MS fuel channels are surrounded by cylindrical graphite sleeves that need to be replaced after reaching their radiation damage limit. The remainder of the reactor is made of non-replaceable graphite, with two horizontal layers of boron-loaded graphite on top and bottom of the reactor to decrease neutron losses. The MS fuel coming out of the core will be regarded as waste. The molten-salt is $NaF + ZrF_4$ + fluorinated actinides; it operates in the temperature range of 600-700°C. The fuel is made by chemically combining light-water reactor spent fuel and its zircaloy cladding with fluorine. UF_6 and the volatile fission products are removed and the remainder is mixed with NaF to form the molten-salt fuel ($NaF + ZrF_4$ with a few per cent TRU). Fresh molten-salt fuel is continuously fed and mixed into the reactor's salt plenum and an equal volumetric flow rate of the mixed molten-salt is continuously removed to keep the overall salt inventory constant. This transmuter is designed to operate as a "once-through" system.

3. Study variables and constraints

The goal of this optimisation study is to maximise the fraction of the actinides fed into the MS reactor that is transmuted in one pass through the reactor while maintaining the design constraints. Four variables are considered for the optimisation study: the pitch of the fuel channels, the diameter of the fuel channels, the volumetric feed and removal rate of the fuel salt, and the concentration of actinides in the feed salt. The composition of the actinide feed in all cases is that shown in Table 1, taken from Bowman. [4]

2. The summary of most of these aspects of the study is adopted from a paper entitled "Optimisation of a Molten-salt Transmuting Reactor" to be presented by the same authors to the PHYSOR-2002 Topical Meeting to be held in Seoul, Korea, a week prior to the Partitioning and Transmutation Information Exchange Meeting.

Table 1. **Actinide feed composition reported in Bowman [4] and used in this study**

Isotope	Feed composition (w/o)	Isotope	Feed composition (w/o)
^{237}Np	4.5	^{241}Am	5.2
^{238}Pu	1.4	^{242}Am	0.0
^{239}Pu	51.5	^{243}Am	0.9
^{240}Pu	23.8	^{244}Cm	0.0
^{241}Pu	7.9	^{245}Cm	0.0
^{242}Pu	4.8	^{246}Cm	0.0

Three constraints are imposed on the design: the power density in the molten-salt, the radiation damage to the graphite, and k_{eff}. Bowman [4] used a power density of 390 watts per cubic centimetre of molten-salt in the core. The same value is used in this study. While there is no solid fuel structure to damage in the MS system, the graphite will swell and may crack as a result of atomic displacements caused by high-energy-neutron collisions. Bowman [4] cites a fast fluence limit of $3x10^{22}$ n/cm^2 of E>0.01 MeV neutrons. The same value is used in this study. Another important constraint the design should be subjected to is the maximum solubility of actinides and fission products in the MS. At the time of the previous study [3] the solubility limit could not have been found by the authors. As a result, this constraint had not been accounted for. Following is the solubility limit data collected so far and used to define the constraint in this paper.

The molten-salts under study contain fluoride – most commonly trifluoride – compounds of actinides (Ac) and lanthanides (La). The fission-product (lanthanide) chemistry in fluoride salts is well understood. Experimental results on the solubility of lanthanide fluorides can be found in ORNL reports and other chemistry journals. [5-8] However, data on actinide fluoride solubilities are scarcer. [9,10] Experimental results show that the solubility of AcF_3 and LaF_3 in molten-salt solvents generally depends on the following factors: (a) ionic radius of Ac^{3+} or La^{3+}, (b) temperature, (c) composition of the molten-salt, (d) type of molten-salt.

Regarding the solubility dependence of AcF_3 and LaF_3 on the ionic radius of the trivalent cations, it has been shown [10] that for the lanthanide trifluorides a lower ionic radius of La^{3+} results in a slightly higher solubility limit of LaF_3; this is illustrated in Figure 1. For actinides, the solubility of AmF_3, CmF_3, BkF_3, CfF_3 has been assumed to be the same as that of PuF_3. [10] Experimental evidence that PuF_3 and AmF_3 have the same solubility in 2LiF-BeF_2 molten-salt can be found in. [9]

As temperature increases, the solubility of Ac and La trifluorides changes at a rate of about 0.5% increase in solubility per one °C increase in temperature. [5]

Changing the composition of the molten-salt also affects the solubility of the trifluoride salts. For NaF-ZrF_4, a higher proportion of ZrF_4 results in significantly increased solubility, as illustrated in Table 2. For example, an increase in ZrF_4 from 50 to 58 mol% results in a change in the solubility limit of CeF_3 from 3.0 to 8.2 mol% at 675°C. However, amounts of ZrF_4 above 50% should be avoided because this component tends to sublimate and later condense inside pipes or pumps causing operational difficulties. [5]

Figure 1. **Dependence of the solubility limits of lanthanide and actinide trifluorides on the ionic radius of Ac^{3+} and La^{3+}, in $NaF\text{-}ZrF_4$ and in $2LiF\text{-}BeF_2$** [10]

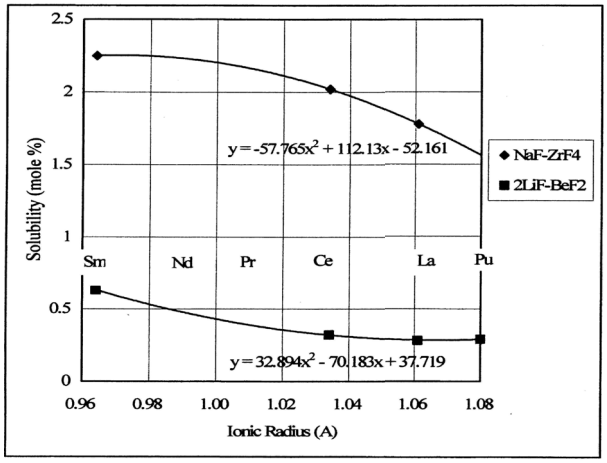

Table 2. **Dependence of the solubility limits of CeF_3 on the temperature and composition of the $NaF\text{-}ZrF_4$ molten-salt** [7]

Solvent comp. (mol%)	**Mol% CeF_3 550°C**	**675°C**	**800°C**
$NaF - ZrF_4$			
42 – 58	3.0	8.2	10.3
50 – 50	2.12	3.0	4.4
53 – 47	1.64	2.37	3.9
59 – 41	0.56	0.62	1.61
63 – 37	0.26	0.44	1.07

The following expressions have been suggested [10] to estimate the solubility at 550°C of different elements in terms of the cation radius:

- in $NaF\text{-}ZrF_4$, solubility (mol%) = $-57.765x^2 + 112.13x - 52.161$;
- in $2LiF\text{-}BeF_2$, solubility (mol%) = $32.894x^2 - 70.183x + 37.719$

where x is the ionic radius of Ac^{3+} or La^{3+} in angstroms.

For this study, the solubility limit of a mixture of only actinides dissolved in $NaF\text{-}ZrF_4$ is taken to be that of the PuF_3, that is, 1.56 mol% at 550°C. The MS operating temperatures considered in the present work are assumed to be between 600°C and 700°C. Using experimental data on temperature dependence of the solubility of PuF_3, [9] the solubility of the AcF_3 in $NaF\text{-}ZrF_4$ at 600°C is estimated as 2 mol%. Hence, the constraint of 1.56 mol% actinides adopted for this work is conservative.

4. Model for analysis

The thrust of the analysis is to find the equilibrium actinides concentration that will be established in the MS reactor characterised by a given set of design parameters and then to analyse the equilibrium reactor characteristics of interest. The equilibrium concentration is found iteratively starting with a

guessed composition. MCNP [11] is run with the composition for a particular geometric configuration to provide the total average neutron flux and the effective one-group cross sections for all the reactions of interest. Using these MCNP-generated data, a coupled set of isotope balance equations is solved to give a new equilibrium composition. If this equilibrium composition is significantly different from the composition used in the MCNP run, then MCNP is run with the new composition and the procedure is repeated until the composition stabilises.

At equilibrium, the actinides concentrations in the MS are to obey the following condition:

$$0 = \sum_j \sigma_{j\to i}\, \phi\, N_j/2 \; + \; \sum_j \lambda_{j\to i}\, N_j \; - \; \lambda_i\, N_i \; - \; \sigma_i\, \phi\, N_i/2 \; + F_i \; - \; R\, N_i \qquad (1)$$

where N_i is the concentration of the i^{th} actinide out of the 27 considered, in units of mol/cm^3, F_i (mol/cm^3-s) is the rate of feed of the i^{th} constituent per unit volume of molten-salt, R (s^{-1}) is the fractional rate of removal of molten-salt from the reactor, σ_i is the effective one-group absorption cross section of the i^{th} constituent, $\sigma_{j\to i}$ is the effective one-group cross section for conversion of actinide j into actinide i, ϕ is the energy-integrated volume-averaged neutron flux in the MS in the core and λ's are decay constants. The factor of 2 dividing the flux terms accounts for the fact that the MS is exposed to the neutron flux only approximately one half of the time, when the MS is flowing through the core; in the other half it circulates through heat exchangers. The actinides are assumed to be mixed uniformly throughout the MS. The 27-by-27 matrix defined by the set of Eqs. (1) is solved numerically using MATLAB.

The fractional transmutation of a particular radionuclide is defined as:

$$T_i \; = \; (N_{i,\,feed} \; - \; N_{i,\,equil})/N_{i,\,feed} \; = \; 1 \; - \; (N_{i,\,equil}\,/\,N_{i,\,feed}) \qquad (2)$$

where $N_{i,\,feed}$ and $N_{i,\,equil}$ are the concentrations of the i^{th} actinide in units of mol/cm^3 in the feed and at equilibrium, respectively.

The 27 nuclides in the chain are isotopes of the elements Np through Cf, where the atomic mass number A is between 237 and 250, with half-lives of days or more. In the case of ^{242}Am, both ^{242g}Am and ^{242m}Am are included in this model. The branching ratio of the neutron capture reaction of ^{241}Am in the thermal energy spectrum is taken to be 0.914 for conversion into ^{242g}Am and 0.086 for conversion into ^{242m}Am. [12]

The MCNP calculations are performed for heterogeneous unit cells in an infinite lattice as depicted in Figure 2. The unit cell is 400 cm high, heterogeneous and hexagonal. The cell is capped at top and bottom by a layer of boron-loaded graphite (see Figure 2). The graphite sleeve is replaceable. This simple model gives a good representation of the core; it only ignores the radial leakage and, in case of an accelerator-driven system, also the source effect. The density used for graphite and MS is, respectively, 2.194 g/cm^3 and 3.1855 g/cm^3. The values of all the cross sections used by MCNP are evaluated at 900 K, the closest to the 650°C average operating temperature of the reactor.

The flux amplitude is determined to provide a constant power density of 390 W/cm^3 of molten-salt in the core, using the following expression:

$$\phi\left(\frac{\text{n}}{\text{cm}^2\text{-s}}\right) = \frac{\text{Power density (W/cm}^3\text{ of MS in core)}}{\sum_i \left\{ \frac{\text{Energy}}{\text{fission}}\left(\frac{\text{J}}{\text{fission}}\right)\Big|_i \; \sigma_{f,i}\,(\text{barn})\; N_i\left(\frac{\text{atoms}}{\text{barn-cm}}\right)\right\}} \qquad (3)$$

$$\left.\frac{\text{Energy}}{\text{fission}}\left(\frac{\text{J}}{\text{fission}}\right)\right|_i = 1.60219 \times 10^{-13}\left(\frac{\text{J}}{\text{MeV}}\right) * \left.\frac{\text{Energy}}{\text{fission}}\left(\frac{\text{MeV}}{\text{fission}}\right)\right|_i \quad (4)$$

$$\left.\frac{\text{Energy}}{\text{fission}}\left(\frac{\text{MeV}}{\text{fission}}\right)\right|_i = 1.29927 \times 10^{-3}\,(Z_i^{\,2} A_i^{\,0.5}) + 33.12 \quad (5)$$

In Eqs. (3)-(5), $\sigma_{f,\,i}$ is the effective one-group fission cross section of the i^{th} actinide and N_i the concentration of this actinide in the appropriate units (atoms/barn-cm). Also, Z_i and A_i are the atomic number and the atomic mass number of the fissioning nuclide i, respectively. [13]

In order to achieve convergence in the iterations that led to the equilibrium points, it was necessary to run at least 1.2 million particle histories in each MCNP run. With fewer particles, the errors in the cross sections and k_{eff} evaluation were larger than the variations of these parameters between subsequent iterations. Each equilibrium point was the result of around ten iterations on average; the difference in k_{eff} from one iteration to the next was observed to decrease monotonically, and convergence was assumed to occur when this difference was <~0.5%.

Figure 2. **Configuration of a unit cell used to model the graphite-moderated MS reactor in MCNP**

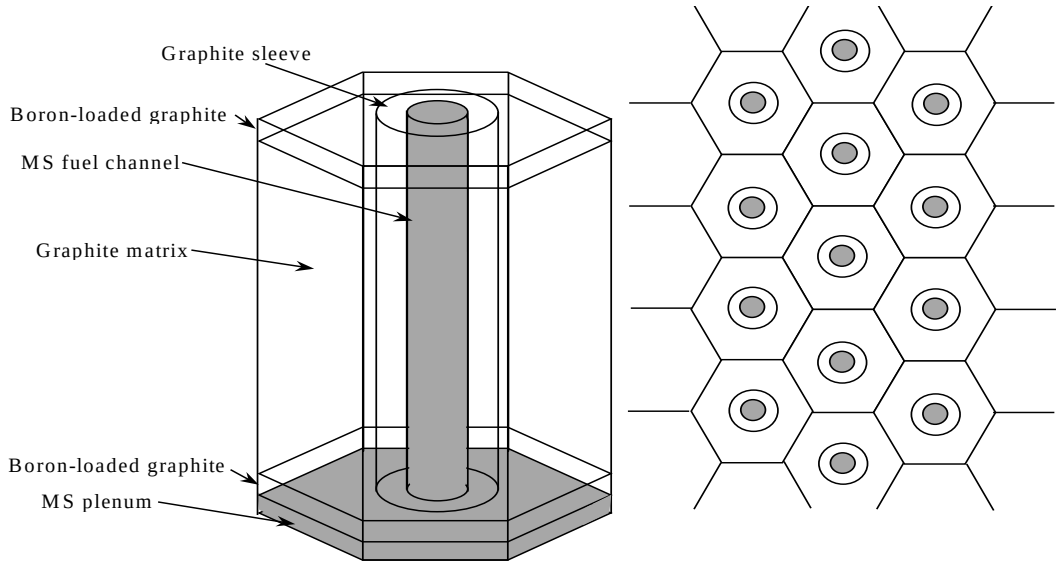

Note that there is a MS plenum also at the top that was not depicted so as to make the figure clearer

5. Results

5.1 Optimal design

All the results reported below pertain to a MS volumetric feed rate of 0.8 litres/day and to an Ac feed concentration of 12.87 mol%. Figure 3 shows the evolution of k_{eff} with the graphite-to-fuel volume ratio (C/MS) ranging from zero – the limit of a homogeneous reactor composed only of molten-salt and actinides – up to C/MS ~20, for the three different fuel channel diameters considered. The 7 cm diameter fuel channel provides the maximum k_{eff} value of 1.03; it is reached at C/MS ~1. The maximum attainable k_{eff} drops slightly and the corresponding C/MS ratio increases as the MS channel diameter becomes smaller. Radial leakage will reduce k_{eff} by a few percent, possibly to the vicinity of unity.

Figure 3. **Dependence of k_{eff} on graphite-to-fuel ratio (C/MS) for different fuel channel diameters**

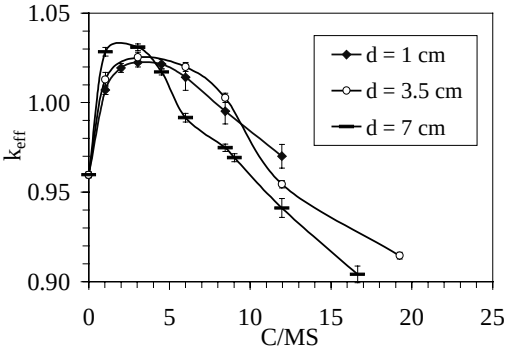

Figure 4. **Dependence of Ac equilibrium concentration (mol%) on graphite-to-fuel ratio (C/MS) for different fuel channel diameters**

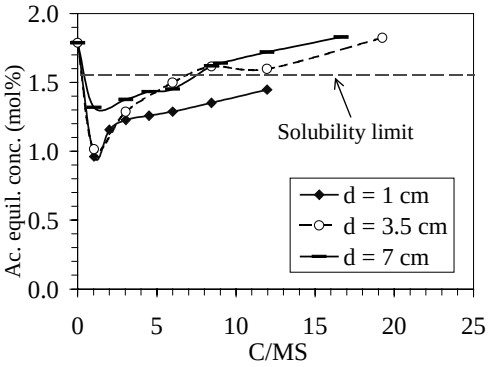

Figure 4 shows the dependence of the equilibrium actinides concentration on the C/MS ratio and MS channel diameter. The minimum equilibrium concentration is obtained for C/MS ratio close to 1.0; that is, corresponding to nearly peak k_{eff}. The minimum equilibrium concentration is well below the solubility limit of 1.56 mol%. The lowest equilibrium concentration of ~0.9 mol% is obtained for d = 1 cm. It gets to ~1 mol% for d = 3.5 cm and to ~1.3 mol% for d = 7 cm. The acceptable C/MS design range for the d = 1 cm channels is significantly larger than for the d = 3.5 cm and 7 cm channels.

Figure 5. **Actinide transmutation efficiency for different fuel channel diameters and graphite-to-fuel ratios (C/MS)**

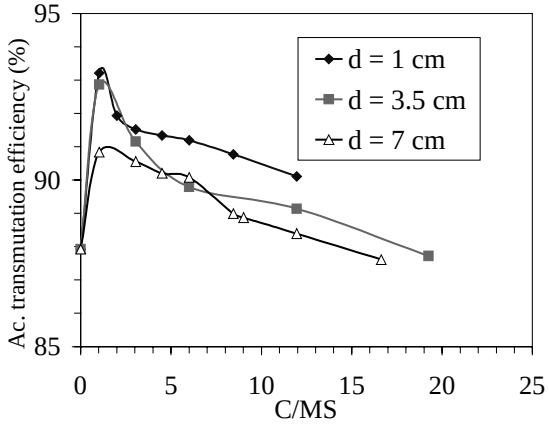

Figure 6. **Normalised total flux in 1 cm diameter fuel channels for C/MS = 1 (epithermal spectrum) and C/MS = 12 (thermal spectrum)**

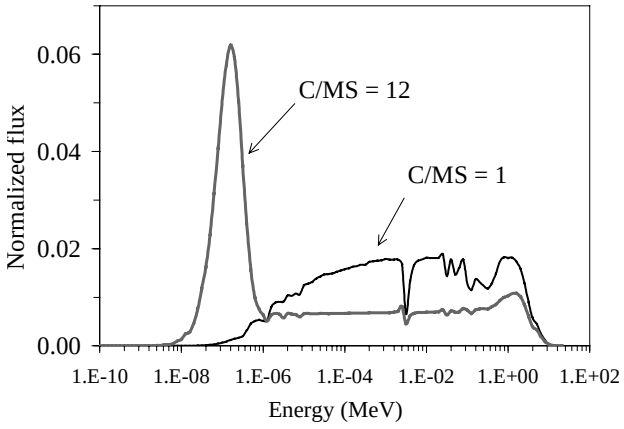

Figure 5 shows the fractional transmutation of actinides at equilibrium. It exceeds 90%, with the smaller MS channel design offering a higher fractional transmutation. A peak Ac transmutation efficiency is reached at C/MS = 1.0 for all of the fuel channel diameters, and its maximum value of 93% is achieved for the case of 1 cm diameter fuel channels.

Measured by each one of the three important performance characteristics: k_{eff}, equilibrium Ac concentration and fractional transmutation, the optimal C/MS ratio is in the vicinity of 1.0. What physical phenomena are responsible for this fortunate situation?

5.2 Neutron balance and spectrum

Figure 6 shows – for the case of 1 cm channel diameter – that the neutron energy spectrum ranges from well-thermalised for C/MS = 12 to highly epithermal for the optimum C/MS of 1. Half of the fissions in the C/MS = 12 system occurred by neutrons with energies of less than 0.15 eV, while in the C/MS = 1 system half of the fissions occurred by neutrons with energies of less than 5 eV. Both neutron energy spectra – and especially the epithermal case – show minima of neutron flux for particular values of the neutron energy. The minimum value of the flux that occurs at 3 keV coincides with a strong resonance in the Na total cross section. Subsequent minimum values of the flux at 30 and 50 keV correspond mainly to resonances in fluorine.

Figure 7 shows the C/MS dependence of the equilibrium composition of different actinides in the 1 cm channel core while Figure 8 shows the corresponding information for the 7 cm channel core. It is observed that in a thermal spectrum core (C/MS = 12) the concentrations of ^{242}Pu and ^{244}Cm are particularly high; they make up approximately 60% of the actinides. As the spectrum hardens their relative concentration declines down to a minimum of ~20% at a C/MS ratio of ~1.0. A reverse trend is observed for the two dominant fissile isotopes: ^{239}Pu and ^{241}Pu. Their concentration increases from approximately 10% to nearly 35% as C/MS is reduced from 12 to 1.0. The outcome is that the ratio of fissile to fertile isotopes peaks in the vicinity of C/MS = 1.0.

Figure 7. **C/MS dependence of the equilibrium composition (atom%) of individual actinides in 1 cm channel**

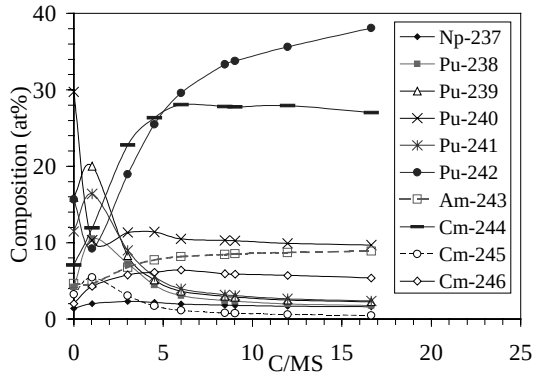

Figure 8. **C/MS dependence of the equilibrium composition of individual actinides (atom%) in 7 cm channel**

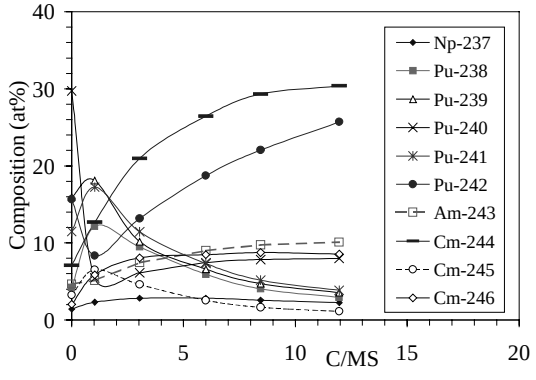

An indication on the reasons for this trend is provided by the C/MS dependence of the absorption probability of selected actinides shown in Figures 9 through 13; the absorption probability (in units of second^{-1}) is calculated as the product of the effective one-group absorption cross section of the actinide times the neutron flux. It is observed that the absorption probability peaks in the vicinity of C/MS = 1.0 for ^{240}Pu, ^{242}Pu and ^{244}Cm. This peak occurs when the neutron spectrum is highly epithermal (Fig 6); it is responsible for the minimum in the concentration of these isotopes (Figures 7 and 8). It is also observed that the absolute value of the peak absorption probability strongly depends on the channel diameter; the smaller the channel diameter the larger is the absorption probability. This is due to resonance self-shielding effects.

On the other hand, the absorption probability of the primary fissile isotopes – ^{239}Pu and ^{241}Pu (Figures 12 and 13) – monotonously increases with C/MS. As a result, the concentrations of ^{239}Pu and ^{241}Pu tend to increase as C/MS goes down to ~1. For C/MS below 1.0 the concentration of ^{240}Pu is increasing so strongly due to a steep decline in its absorption probability that the relative concentrations of ^{239}Pu and ^{241}Pu drop.

Figure 14 summarises the overall neutron balance for the systems with 1 cm channels considered. k_{inf} peaks in the vicinity of C/MS = 3 due, primarily, to a minimum in the parasitic neutron capture in the non-fuel constituents of the MS and to a reduction, with decrease in C/MS, in the parasitic neutron capture in graphite. The relatively low parasitic neutron capture near C/MS = 3 more than compensates for the relatively low fuel reactivity as measured by the average η of the actinides. As the leakage probability is at a minimum in the vicinity of C/MS = 3, where k_{inf} peaks, k_{eff} peaks also at C/MS = 3 (Figure 3).

Figure 9. **Absorption probability of ^{240}Pu**

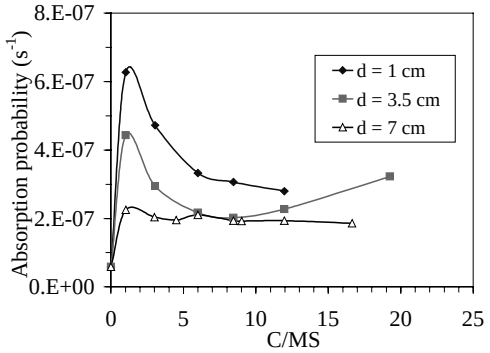

Figure 10. **Absorption probability of ^{242}Pu**

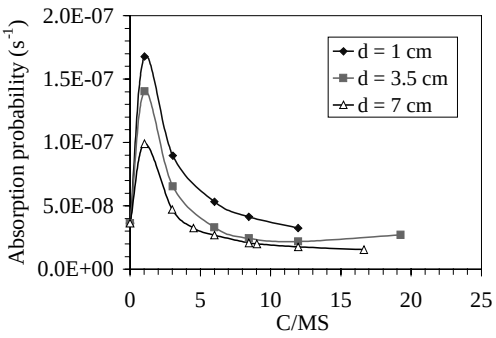

Figure 11. **Absorption probability of ^{244}Cm**

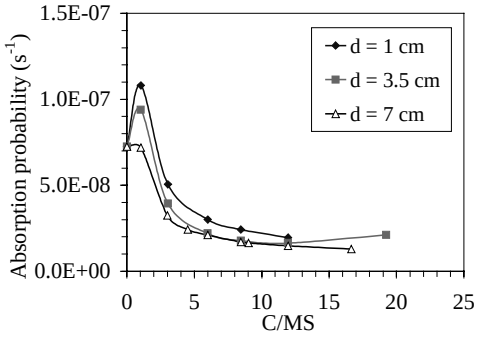

Figure 12. **Absorption probability of ^{239}Pu**

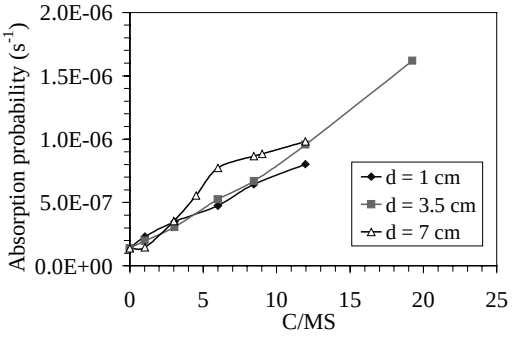

Figure 13. **Absorption probability of ^{241}Pu**

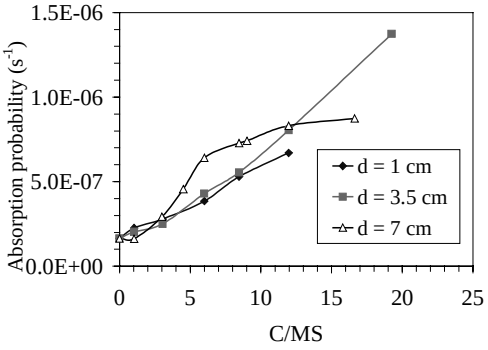

Figure 14. **Neutron balance and k_{inf} for 1 cm fuel channels and different C/MS value**

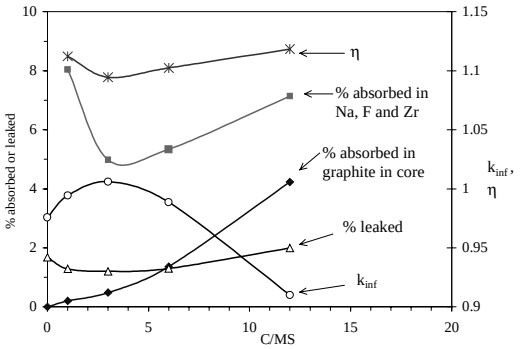

5.3 Graphite lifetime

Figure 15 shows the graphite sleeve lifetime strongly depends on the C/MS ratio; the smaller this ratio the shorter is the lifetime. For C/MS = 1 the lifetime is less than one year; too short to be practical. The reason for the short lifetime of the graphite is the increase in the fast neutron flux amplitude with spectrum hardening due to a reduction in C/MS ratio, as shown in Figure 16. This is due to a reduction in the effective one-group fission cross section. It is possible to increase the graphite lifetime while retaining the C/MS ratio of 1.0 by lowering the power density of the molten-salt in the core. For example, at 39 W/cm^3 of molten-salt (one-tenth of the original power density), the lifetime of the graphite increases from 0.6 to 5.7 years as the total flux in the fuel region decreases by about one order of magnitude, while k_{eff} drops to 0.952 and the equilibrium actinide concentration increases to 1.4 mol% – still within the k_{eff} and solubility limit constraints. For C/MS = 3.0, the graphite lifetime reaches 12 years at 39 W/cm^3 power density (Table 3).

Figure 15. **C/MS dependence of graphite sleeve lifetime (years)**

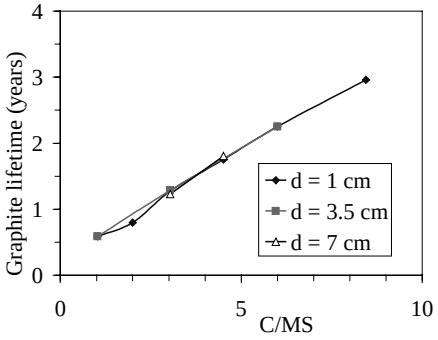

Figure 16. **C/MS dependence of total flux in the fuel region**

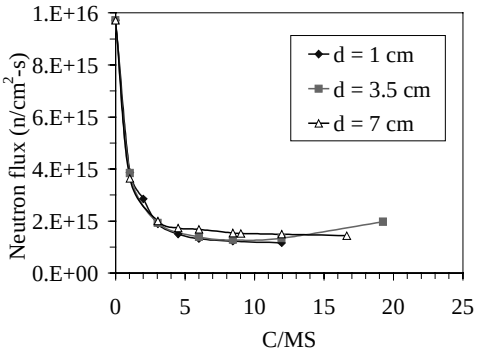

Table 3. **Effect of reducing the power density on the transmuter performance**

Power density	**C/MS = 1.0**		**C/MS = 3.0**	
	390 W/cm^3	39 W/cm^3	390 W/cm^3	39 W/cm^3
k_{eff}	1.007	0.952	1.023	0.958
Equilibrium Ac concentration (mol%)	0.96	1.40	1.23	1.60
Ac fractional transmutation (%)	93.21	90.45	91.22	89.28
Flux in fuel region (n/cm^2-s)	3.87x10^{15}	3.82x10^{14}	1.89x10^{15}	1.90x10^{14}
Graphite lifetime (yr)	0.59	5.7	1.28	12

The unfortunate decline in k_{eff} with a reduction in the power density or flux amplitude is due to a reduction in the fission probability of short-lived actinides such a ^{238}Np. With a half-life of only 2.117 days, the probability that the ^{238}Np will decay into ^{238}Pu rather than fission before decaying gets higher as the flux amplitude decreases. The created ^{238}Pu is more likely to capture a neutron than to fission, thus consuming an extra neutron and lowering the k_{eff} relative to a higher flux reactor. On the other hand, higher flux is expected to somewhat increase the negative reactivity effect of those fission products that can not be removed from the MS short enough after their creation.

5.4 Proliferation Resistance

The proliferation resistance characteristics of the equilibrium molten-salt fuel varies significantly with the C/MS ratio. Figure 17 (also Figures 7 and 8) shows the C/MS dependence of the plutonium isotopic composition. At the high C/MS range the plutonium isotopic composition is unusual among reactor systems in terms of proliferation resistance; it has a relatively low fissile-fuel content. For example, at C/MS = 20, fissile plutonium constitutes only ~9 w/o of the plutonium inventory (for 3.5 cm channel diameter). Table 4 compares the equilibrium MS reactor Pu composition to that in weapons-grade Pu; in spent fuel from a lead-cooled reactor with a long-life core (the Encapsulated Nuclear Heat Source or ENHS); [14] and to the Pu in light-water reactor spent fuel (LWR SF). The C/MS of 12 given in Table 4 is the upper bound dictated by the actinides solubility limit (Figure 4).

Table 4. **Isotopic composition (w/o) of Pu in the MS reactor having 1 cm channels compared to weapons grade Pu, spent fuel from the ENHS, and spent fuel from a LWR**

	Type of Pu				
	Weapons Grade	ENHS (EOL)	LWR SF	Molten salt reactor C/MS =1	Molten salt reactor C/MS =12
^{238}Pu	0	0.3	1.6	19	7
^{239}Pu	94	70.5	57.6	31	8
^{240}Pu	6	22.3	26.6	9	18
^{241}Pu	0	2.7	8.8	28	9
^{242}Pu	0	4.2	5.4	13	58
Total fissile	94	73.2	66.4	59	17

Figure 17. **Pu isotopics dependence on C/MS ratio; 1 cm diameter channel**

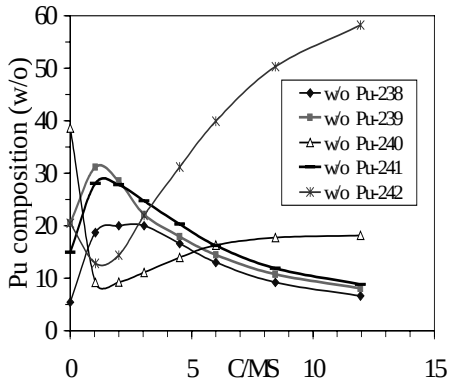

5.5 Illustration

In the following we'll choose a set of design variables that may lead to a well performing reactor. First consider the power density. We'll chose the high value of 390 W/cm^3 of MS since the higher is the power density the better becomes the neutron balance (higher k_∞; Table 3) and the lower will be the specific investment ($/kW$_{installed}$). For the C/MS ratio we'll chose 3 since it offers ~twice as long a graphite life than C/MS = 1 (Table 3) and nearly maximum k_{eff} (Figure 3) with well acceptable equilibrium concentration (Figure 4) and fractional transmutation (Figure 5). For the channel diameter we'll chose 7 cm as it offers the highest k_{eff} of 1.032 (Figure 3; not accounting for radial leakage) and large enough pitch to provide a graphite structure that is reasonably thick (close to 7 cm) in between MS channels. What remains to be selected are the core dimensions.

The core height-to-diameter (H/D) ratio is chosen to be 0.924; this is what a simple one-group diffusion theory predicts to give the lowest neutron leakage probability for a given core volume. There remains to choose the core volume or total core power. The axial leakage probability from a 4 m tall core is calculated to be approximately 1% (Figure 14 for C/MS=3). The corresponding radial leakage probability for a core that is (4/0.924=) 4.33 m in diameter is estimated to be 2%. This makes k_{eff} of (~1.032-0.02=) 1.01. The extra 1% may be sufficient to compensate for the reactivity effect of fission products, provided that Xe and other volatile fission products are immediately removed, and of the delayed neutrons that are emitted while the MS is out of the core. The total power of this core will be 5 740 MW_{th}. By going to 10 000 MW_{th} per core, the neutron leakage probability will be reduced by almost 1% thus providing some extra reactivity margin to compensate for the reactivity effect of

fission products and lost delayed neutrons. Since the MS reactor is not pressurised and its passive safety does not depend on the core surface-to-volume ratio, we see no compelling reason against the high power level per core.

There is though a drawback in high power density – short graphite lifetime. This drawback can be overcome by designing two side-by-side cores in one plant. When the graphite in one core reaches its radiation damage limit, this core is shut down and the MS from this core is pumped into the other core that has fresh graphite. After the core with the fresh graphite is brought to full power operation, the graphite in the other core will be replaced. As the time required for pumping the MS from one core to the other is on the order of few days, the availability of the dual core power plant could be very high. As the dual core plant will have only one set of heat exchangers and BOP, the addition of a second core is not likely to have a large economic penalty; it is likely to be more economical than designing a single core having a significantly lower power density.

6. Discussion

If fission products are not removed from the reactor as assumed in this study, the attainable k_{eff} will be lower than that reported above. Fortunately, xenon and the other volatile fission products will get out of the MS shortly after their production. This, combined with the use of an epithermal spectrum, will reduce the reactivity effect of fission products relative to their effect in thermal solid fuel reactors. AS the Xe residence time in the core is expected to be on the order of seconds, its reactivity effect can be neglected. An upper bound on the reactivity effect of Sm is ~0.5% – the yield of ^{149}Pa per fission neutron. The reactivity effect of the longer life fission products is not likely to exceed 0.5%, especially if fission products will slowly be removed by on-line processing of a side stream of MS. Thus we anticipate that the overall reactivity effect of fission products will not exceed 1%. The fission product effect will be quantified accurately in a follow-on study.

In calculating k_{eff} we ignored the fact that a fraction of the delayed neutrons will be emitted when the MS is outside of the core. Assuming that the MS volume in the core and out of the core are the same, the loss in reactivity due to out of core decay of delayed neutron precursors is estimated to be 0.5β. Assuming that the average delayed neutron fraction of the equilibrium actinides is in the vicinity of $\beta = 0.004$, the negative reactivity effect due to loss of delayed neutrons is expected to be ~0.2%.

The actual fuel feed composition will be different from that assumed for this study (Table 1); it will include some ^{238}U and other U isotopes that cannot be completely separated from the TRU. Sensitivity analysis we recently did showed, though, that the MS reactor performance reported in this work will practically not change when using for the feed the composition recommended [15] for the use by the AAA project. This composition is ^{237}Np – 6.641 w/o; ^{238}Pu – 2.749; ^{239}Pu – 48.652; ^{240}Pu – 22.980; ^{241}Pu – 6.926; ^{242}Pu – 5.033; ^{241}Am – 4.654; ^{242m}Am – 0.019; ^{243}Am – 1.472; ^{242}Cm – 0.0; ^{243}Cm – 0.005; ^{244}Cm – 0.496; ^{245}Cm – 0.038; ^{246}Cm – 0.006 $^{w}/_{o}$. The total fissile contents is 55.6 $^{w}/_{o}$.

7. Conclusions

It is scientifically feasible to design a NaF-ZrF_4 MS reactor that is fed by transuranics from LWR spent fuel and that operates at an average power density of 390 W/cm^3 of MS in the core to have an equilibrium k_{eff} that is 1.0, provided the fission products poisoning can be maintained at up to 1% in reactivity and provided the core is large – on the order of 10 GW_{th} in power. Smaller cores could be designed to be sub-critical driven by an accelerator. In either design approach k_{eff} can be maintained constant throughout the core life after the actinides reached their equilibrium concentration.

The fractional transmutation of the MS reactors is exceptionally high – it can exceed 90%. k_{eff} peaks in the C/MS range between 1 and 5. The fractional transmutation has a peak in the vicinity of C/MS of 1.0. The equilibrium actinide concentration is at a minimum for this C/MS ratio; it is well below the solubility limit. The optimal core has an epithermal spectrum that maximises the absorption cross-section of ^{242}Pu and ^{244}Cm and thus minimises their concentration. Due to reduced spatial self-shielding, small channel diameters offer higher fractional transmutation and lower equilibrium concentration than large channel diameters; the peak k_{eff} is only slightly sensitive to the channel diameter. The maximum C/MS ratio acceptable for 1 cm diameter channels is above 12; almost double than that for the 3.5 and 7 cm diameter channels. At C/MS = 12, fissile isotopes constitute only 17 w/o of the plutonium. The graphite lifetime of this reactor is only of the order of one year. It is possible to increase the lifetime by reducing the power density. Reduction of the power density to 39 W/cm^3 can increase the graphite lifetime to ~10 years. Lowering the power density will somewhat reduce the attainable k_{eff} and increase the equilibrium actinide concentration.

More thorough analyses are required before the feasibility of the MS transmuting reactor could be reliably assessed. One of the primary issues that need to be addressed is the effect of non-instantaneous removal of the fission products. Another issue is what it takes to get to the equilibrium composition. Practical designs of MS reactors that take into account the radiation damage of the graphite need to be worked out.

Acknowledgement

This work was supported by the U.S. Department of Energy Office of Nuclear Energy, Science, and Technology through the Los Alamos National Laboratory under contract number 14631-001-00 2K.

REFERENCES

[1] G.J. van Tuyle and D.E. Beller (1999), *Accelerator Transmutation of Waste Technology and Implementation Scenarios*, Proceedings 3rd Int. Topical on Nuclear Applications of Accelerator Technology, Long Beach, CA.

[2] M.D. Lowenthal and E. Greenspan (2001), *Parametric Studies for Optimization of a Graphite-Moderated Molten-salt Transmuter,* Proceedings of the Global 2001 Conference, Paris, France, September.

[3] E. Greenspan, M. Lowenthal, D. Barnes, D. Kawasaki, D. Kimball, H. Matsumoto, H. Sagara and E.R. Vieitez (2001), *Transmutation Capability of a Once-through Molten-salt and Other Transmuting Reactors*, Proceedings of Topical Mtg. on Accelerator Applications, Reno, NV, November.

[4] C.D. Bowman (2000), *Once-through Thermal-spectrum Accelerator-driven LWR Waste Destruction Without Reprocessing*, Nuclear Technology, 132, pp. 66-93, October.

[5] J.A. Lane, H.G. MacPherson and F. Maslan (1958), *Fluid Fuel Reactors*, Addison-Wesley Publishing Company, Reading, Massachusetts, USA.

[6] W.R. Grimes, J.H. Shaffer, N.V. Smith, R.A. Strehlow, W.T. Ward and G.M. Watson (1959), *High-temperature Processing of Molten Fluoride Nuclear Reactor Fuels*, Chemical Engineering Progress Symposium Series Part VII, No. 27, Vol. 55, p. 65.

[7] W.T. Ward, R.A. Strehlow, W.R. Grimes and G.M. Watson (1960), *Rare Earth and Yttrium Fluorides: Solubility Relations in Various Molten NaF-ZrF_4 and NaF-ZrF_4-UF_4 Solvents*, J. Chem. and Eng. Data, 5(2), pp. 137-142.

[8] M.W. Rosenthal, P.N. Haubenreich and R.B. Briggs (1972), *Molten-salt Reactor Program: The Development Status of Molten-salt Breeder Reactors*, Oak Ridge National Laboratory Report ORNL-4812.

[9] J.C. Mailen, F.J. Smith and L.M. Ferris (1971), *Solubility of PuF_3 in Molten 2 LiF-BeF_2*, J. Chem. & Eng. Data, 16 (1), pp. 68-69.

[10] Y. Hirose and Y. Takashima (2001), *The Concept of Fuel Cycle Integrated Molten-salt Reactor for Transmuting Pu+MA from Spent LWR Fuels*, Proceedings of the Global 2001 Conference, Paris, France, September.

[11] J.F. Briesmeister (1997), ed. *MCNP – A General Monte Carlo Code N-Particle Transport Code Version 4B*, Los Alamos National Laboratory Report LA-12625-M, Version 4B.

[12] G. Fioni *et al.* (2001), *Incineration of ^{241}Am Induced by Thermal Neutrons*, Nuclear Physics A 693, pp. 546-564.

[13] A.G. Croff (1983), *Origen 2: A Versatile Computer Code for Calculating the Nuclide Compositions and Characteristics of Nuclear Materials*, Nuclear Technology, 62, pp. 335-352.

[14] E. Greenspan, H. Shimada and K. Wang (2000), *Long-life Cores with Small Burn-up Reactivity Swing*, Proceedings of the 2000 Int. Topical Mtg. on Advances in Reactor Physics and Mathematics and Computation into the Next Millennium, PHYSOR-2000, Pittsburgh, PA.

[15] Table 5.2 of *Candidate Approaches for an Integrated Nuclear Waste Management Strategy – Scoping Evaluations*, Los Alamos Report LA-UR-01-5572, Nov. 2001.